SCIENTIFIC REPORTS

OPEN

Filling the gaps of dinosaur eggshell phylogeny: Late Jurassic Theropod clutch with embryos from Portugal

Ricardo Araújo[1,2], Rui Castanhinha[2,3], Rui M. S. Martins[2,4,5,6], Octávio Mateus[2,7], Christophe Hendrickx[2,7], F. Beckmann[8], N. Schell[8] & L. C. Alves[4,6]
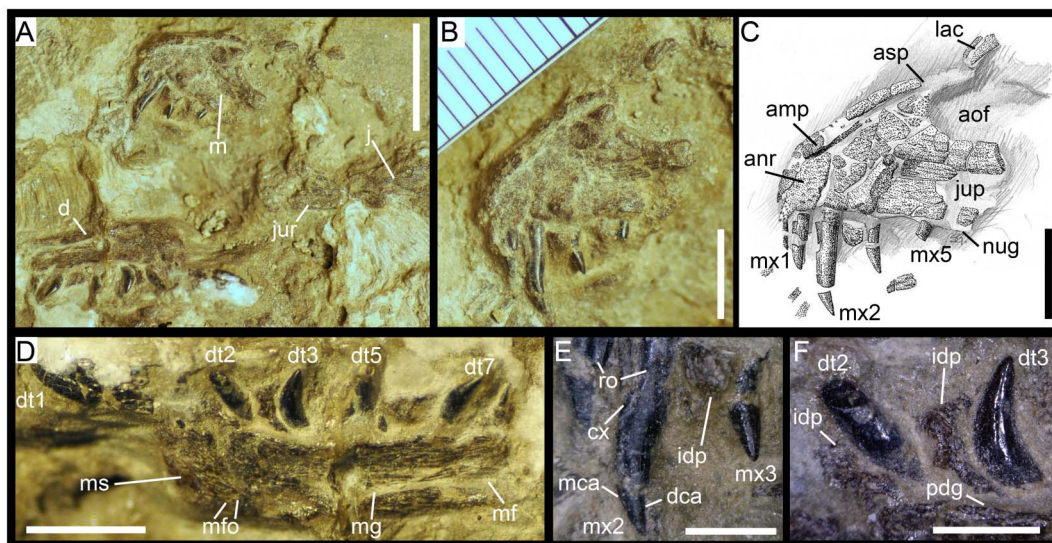
[1]Huffington Department of Earth Sciences, Southern Methodist University, Dallas, Texas, 75275-0395, [2]Museu da Lourinhã, Rua João Luis de Moura, 95, 2530-158 Lourinhã, Portugal, [3]Instituto Gulbenkian de Ciência, Rua da Quinta Grande, 6P-2780-156 Oeiras, Organogenesis Ibn Batuta (A1) - Room 1A, Portugal, [4]IST/CTN, Campus Tecnológico e Nuclear, EN10, 2696-953 Sacavém, Portugal, [5]CENIMAT/I3N, Faculdade de Ciências e Tecnologia da Universidade Nova de Lisboa, Quinta da Torre, 2829-516 Caparica, Portugal, [6]Centro de Física Nuclear da Universidade de Lisboa (CFNUL), Av. Prof. Gama Pinto 2, 1649-003 Lisboa, Portugal, [7]CICEGe, Centro de Investigação em Ciência e Engenharia Geológica, Faculdade de Ciências e Tecnologia da Universidade Nova de Lisboa, Quinta da Torre, 2829-516 Caparica, Portugal, [8]Helmholtz-Zentrum Geesthacht (HZG), Max-Planck-Str. 1, 21502 Geesthacht, Germany.

The non-avian saurischians that have associated eggshells and embryos are represented only by the sauropodomorph *Massospondylus* and Coelurosauria (derived theropods), thus missing the basal theropod representatives. We report a dinosaur clutch containing several crushed eggs and embryonic material ascribed to the megalosaurid theropod *Torvosaurus*. It represents the first associated eggshells and embryos of megalosauroids, thus filling an important phylogenetic gap between two distantly related groups of saurischians. These fossils represent the only unequivocal basal theropod embryos found to date. The assemblage was found in early Tithonian fluvial overbank deposits of the Lourinhã Formation in West Portugal. The morphological, microstructural and chemical characterization results of the eggshell fragments indicate very mild diagenesis. Furthermore, these fossils allow unambiguous association of basal theropod osteology with a specific and unique new eggshell morphology.

The discovery of fossilized eggs and embryos together is rare[1–3]. Eggshells associated with non-avian saurischian embryos are reported for (i) the Early Jurassic sauropodomorph *Massospondylus*[4], (ii) the Late Jurassic avetheropod *Lourinhanosaurus*[5,6], (iii) a Late Cretaceous therizinosauroid[7], (iv) Early and Late Cretaceous titanosaurs[8], (v) the Late Cretaceous troodontids[9,10], and (vi) a Late Cretaceous oviraptorid[11]. Thus, there is a dearth of knowledge regarding eggs associated with embryos at the base of Saurischia, especially prior to the Late Cretaceous. Fossil embryos provide important information about (i) ontogenetic transformations including heterochronic processes[12], (ii) developmental pathways in multiple lineages[13], (iii) reproductive behaviors including parental care[14], and (iv) the evolution of physiological regimes[15]. Yet, studies on embryo osteology are particularly difficult because species-level identification is often hampered by poor ossification of the specimens, which can result in a paucity of diagnostic anatomical features[11]. The purpose of this paper is to link a new eggshell morphology to the osteology of a particular group of basal theropod dinosaurs, as well as to evaluate the extension of diagenesis on the morphology of the eggshell. We employed synchrotron radiation-based micro-computed tomography (SR-μCT), scanning electron microscopy (SEM), and optical microscopy techniques to study the morphology and microstructure of the eggshell fragments (see Methods). Additionally, eggshells and surrounding sediment characterization was performed by using an array of complementary techniques in order to assess the extension of diagenesis, namely micro-Proton Induced X-ray Emission (micro-PIXE), Synchrotron radiation-based X-Ray Diffraction (SR-XRD) and cathodoluminescence (CL) (see Methods and Supplementary Notes).

Results

Discovery. The specimen (ML1188, ML – Museu da Lourinhã, Portugal) is composed of a large number (> 500) of clustered eggshell fragments forming an assemblage 65 cm in diameter, containing embryonic bones and teeth (Fig. 1; Supplementary Note 1). No other vertebrate remains or eggshell fragments were found in the immediate area. The assemblage was discovered on a grey mudstone layer (39° 13′ N; 9° 20′ W; exact coordinates available

Figure 1 | (a) Right maxilla, dentary and jugal of *Torvosaurus* sp. (ML 1188) in medial view. (b & c) Anterior part of right maxilla of *Torvosaurus* sp. (ML 1188) in medial view. (d) Right dentary of *Torvosaurus* sp. (ML 1188) in medial view. (e) Anteriormost maxillary teeth in medial view. (d) Anteriormost dentary teeth in medial view. Abbreviations: **amp**, anteromedial process; **anr**, anterior ramus; **aof**, antorbital fenestra; **cx**, cervix dentis; **d**, dentary; **d1**, isolated first dentary tooth; **d2**, second dentary tooth; **d3**, third dentary tooth; **d5**, fifth dentary tooth; **dt7**, seventh dentary tooth; **dca**, distal carina; **idp**, interdental plate; **j**, jugal; **jur**, jugal ramus; **lac**, lacrimal contact of the maxilla; **m**, maxilla; **mca**, mesial carina; **mf**, Meckelian fossa; **mfo**, Meckelian foramina; **mg**, Meckelian groove; **ms**, mandibular symphysis; **mx1**,first maxillary tooth; **mx2**, second maxillary tooth; **mx5**, fifth maxillary tooth; **nug**, nutrient groove; **pdg**, paradental groove; **ro**, root. Scale: 10 mm for (a), 5 mm for (b), (c) & (d); 2 mm for (e) & (f).

upon request) in August 2005 by A. Walen at Porto das Barcas in the Sobral Member of the Lourinhã Formation. Excavation was performed in September 2005 and May 2006. A single block containing the entire assemblage was jacketed in the field using a specific technique previously described[16]. The specimen was prepared at the Museu da Lourinhã in 2009. Another clutch (ML565) previously described[5], referred to as the Paimogo nest, was found in penecontemporaneous deposits of the Lourinhã Formation in 1993 by I. Mateus, less than 10 km away from the area where ML1188 was collected. The Paimogo nest was recovered from an iron-rich mudstone layer. Despite the dubious phylogenetic position of the avetheropod *Lourinhanosaurus antunesi*[6,17], the Paimogo nest was tentatively ascribed to this taxon.

Clutch. In spite of post-burial compression[18], the observation of continuous patches of eggshells allows discerning eggshell orientations, which indicate the presence of different eggs. In Supplementary Note 1a the assemblage can be divided into three different mounds: one at the top, one at the middle, and one at the bottom. The top mound has eggshell patches with N-S fracture orientation, whereas the middle and lower mounds E-W fracture patterns. All the eggs are heavily crushed, and individual boundaries between the eggs are difficult to distinguish (Supplementary Note 1). Nevertheless, this assemblage forms a clutch (ML1188) because it consists of several eggs (> 3) mingled with embryonic bones. There are generally one or two eggshells vertically stacked, but rarely three or four eggshells are found piled up (Supplementary Note 1). Embryonic material in the clutch consists of five dispersed and isolated teeth, a maxilla preserving four teeth, a dentary with four teeth *in situ*, an isolated dentary tooth, a series of three articulated centra, and other unidentifiable bones (Fig. 1; Supplementary Note 1, 2, 4, and 6). ML1188 was found as an isolated and concentrated clutch without any surrounding dispersed eggshells.

Embryonic remains. The medial side of the incomplete right maxilla is on the surface of the clutch (Fig. 1, Supplementary Note 2). The partial maxilla comprises the anterior ramus, an incomplete

ascending process, and the jugal ramus whose the posterior part is separated from the rest of the maxillary bone. The main body has a Subtriangular anterior ramus projecting moderately anteriorly from the antorbital fenestra (Fig. 1). The anterior margin of the anterior ramus is convex and forms a right angle with the ventral margin of the maxilla. The anterodorsal margin of the anterior ramus is slightly concave and confluent with the ascending process, thus, there is no step delimiting the two structures. The jugal ramus is broken in two pieces, the posterior part lying one centimeter below the maxilla. Once digitally restored (Supplementary Note 3), the jugal ramus is elongated with some parts in the middle of the ramus missing. The dorsal margin of the horizontal ramus, corresponding to the ventral rim of the antorbital fenestra, is straight and subparallel to the tooth row in its anterior part whereas the posterior part of the ramus has a sigmoid outline and slopes ventroposteriorly towards the jugal contact of the ramus. The posteriormost part of the jugal ramus corresponds to a tongue-like process delimited by a small concavity on its dorsal margin and the main axis passing through this posterior process is oriented ventroposteriorly. The ventral margin of the jugal ramus is straight and parallel to the anteroposterior axis of the jugal process. Little information can be extracted from the jugal but the contact between the jugal and maxilla extends one third on the lateral side of the jugal ramus. The articular surface for the lacrimal is visible on the anteromedial part of the jugal, at the level of the posterior process of the jugal ramus. The lacrimal was also contacting the maxilla along one third of the jugal ramus. The ascending process is thick at its base and tapers dorsally. The anteroventral margin of the ascending process is convex, almost forming an obtuse angle, and the main axis passing through this process angles 28° with the ventral margin of the maxilla. Two elongated and subparallel ridges are present at the dorsal tip of the ascending process and delimit the lacrimal contact of the maxilla. The antorbital fenestra is parabolic in outline. There is no medial antorbital fossa. The medial surface of the maxilla bears parallel stripes corresponding to vascular canals. On the main body of the maxilla, these canals are anteroposterioly aligned but, on the ascending process they are parallel to its main axis. However,
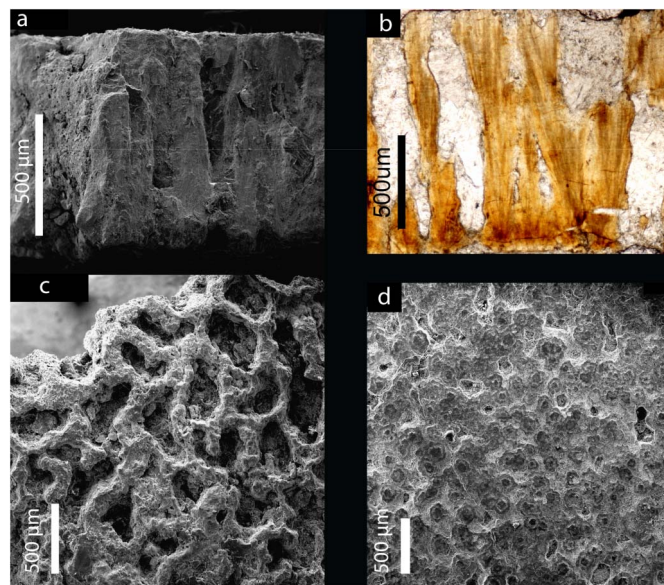
the canals are more irregularly placed on the anterior part of the ascending ramus. Although the anteromedial surface of the maxilla is damaged, the surface is composed of solid bone, thus no maxillary and promaxillary fenestrae, maxillary antrum and pneumatic excavations are present. At the level of the teeth roots, only one isolated interdental plate has been preserved in between the second and fourth maxillary teeth. This suggests that the interdental plates of the maxilla were unfused. The plate is subrectangular, and its surface is punctuated. The anteromedial process has been crushed at the level of the anterior margin of the maxilla. The anteromedial process is located on the anterodorsal border of the anterior ramus, being a long finger-like projection parallel to the anterodorsal rim of the anterior ramus. Four maxillary teeth are preserved on the anterior part of the maxillary body and there is an isolated tooth near the maxilla and two more loose teeth located some distance away from this bone. The maxillary tooth count is difficult to estimate because the posterior part of the main body bears no teeth. However, on the anterior ramus of the maxilla there were probably five teeth. All teeth are strongly elongated (Crown Height Ratio > 2.5), their apices are sharply acute and both mesial and distal carinae lack serrations. The mesial and distal profiles are recurved distally and the crowns are subconical. Nevertheless, the lingual surface of the crowns is mostly flattened except the basal surface which is concave. This concave area on the medial surface of the crown received the erupting tooth of the maxilla. The enamel surface of the teeth is smooth and does not bear transversal undulations, enamel wrinkling, longitudinal grooves, or wear facets.

A right dentary is lying on its lateral side just below the anterior part of the maxilla (Fig. 1, Supplementary Note 4). The bone is almost complete and only part of the bone posterior to the opening of the Meckelian fossa is missing. It is fractured in the middle by a transversal fissure. The dentary is massive, with a ventrodorsally large medial wall remaining the same width along the bone. Four fully erupted teeth are present on the dentary but only two of them, the third and seventh dentary teeth, are complete. A fifth isolated tooth, most likely the first dentary tooth, is lying beside the anteroventral corner of the dentary. Based on the positions of the remaining teeth, we estimate a total of eight alveoli on this portion of the dentary. The interdental plates are unfused. Three interdental plates are preserved in between the first and second dentary teeth, the second and third, and the fifth and seventh teeth. Variation occurs in the shape of the interdental plates along the tooth row as the two anteriormost plates form a vertical rectangle whereas the third one, more posteriorly located, has a horizontal rectangular outline. The mandibular symphysis is short, smooth and forms an elongated triangle on the anteriormost part of the dentary. The paradental groove separating the medial wall of the dentary with the interdental plates is large, gently concave and seems to have been open in between those two structures. The Meckelian groove is well visible on the dentary, running along the bone just above the dorsal margin of the dentary. This longitudinal groove is filled with sediment and seems to extend anteriorly until the third dentary teeth. The step between the Meckelian groove and Meckelian fossa occurs at the level of the seventh dentary tooth. Only the anterior part of the Meckelian fossa is preserved. A large concavity at the level of the third dentary tooth is present just above the ventral margin of the dentary and includes a short anteroposteriorly oriented ridge. Two small grooves located in between this concavity and the mandibular symphysis are interpreted to be Meckelian foramina (Fig. 1). The anteroventral margin of the dentary is rounded and almost subrectangular, with the inflexion point close to the level of the anteriormost point of the dentary. The anteroventral margin is unexpanded with no articular brace forming a chin, and the ventral margin appears to have been fairly straight. The teeth of the dentary are unserrated and the crowns are pointed, strongly basoapically elongated and recurved posteriorly, and devoid of enamel structure.
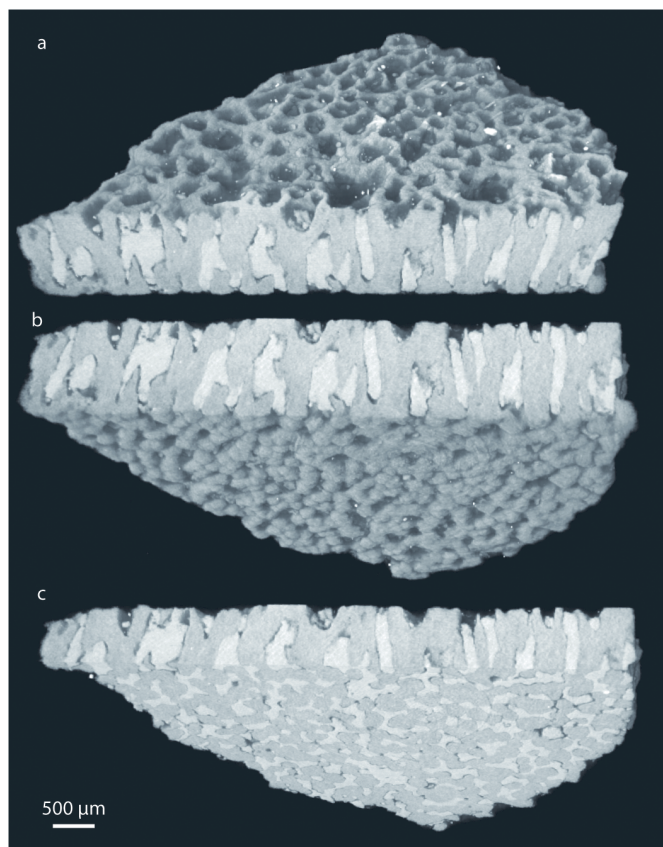
Three articulated amphiplatyan vertebrae were fully prepared (Supplementary Note 6). The ventral part of the centrum bears two paired pits identified as neurovascular foramina. The anterior and posterior faces of the vertebrae show evenly distributed small pits, consistent with an early developmental stage[8]. The centrum faces are expanded ($\sim$ 38% relative to the mid-centrum) and bear confluent striations, whereas in the median part of the centrum, the striations are parallel. Although other fragmentary bones are present and scattered within the clutch none are identifiable, thus, no further information could be obtained.

Eggshell characterization. The total eggshell thickness of the ML1188 eggshells is approximately 1.2 mm. They bear (i) anastomizing ornamentation resembling to some degree the patterns of lineari-tuberculate[1] ornamentation, consisting of sub-circular to sub-elliptical grooves separated by interconnected sharp ridges (Fig. 2c, 3a), (ii) acicular, elongated blade-shaped, calcite crystals radiating from the base of the mammillae to the outermost part of the eggshell (Fig. 2b), and (iii) only one primary layer (Figs. 2a,b, 3a,b). Growth lines are visible across the entire thickness of the eggshells, but tend to be concentrated at the base and develop perpendicularly to the acicular calcite crystals of the wedges (Fig. 2b). The mammillae height, which is difficult to measure for this eggshell morphotype, averages 166 µm, corresponding to about 17% of the total thickness of the eggshell (Figs. 2b, 3b).

The results presented in Fig. 3 show that SR-µCT is a useful technique for non-destructive imaging of the eggshell morphology. The morphology of the pores is provided by high-quality data that is difficult to visualize by SEM or thin-sections. The pores are irregular canals that ramify and vary in width along their length (i.e., resembling prolatocanaliculate[1]). Their diameter is highly variable because the contour is irregular, ranging between $\sim$ 100 µm and 500 µm. Pores anastomose with adjacent pores close to the outer surface (Fig. 2, 3). In fact, the pores seem to form an interconnected system (Fig. 3c and Supplementary videos). All eggshells have equivalent pore density, which indicates that all the eggs were buried under a homogenous incubating medium[19]. Eggshell ornamentation consists of well-defined ridges and islets with prominent and sub-vertical walls, which show no flattening or smoothing of their sharp edges
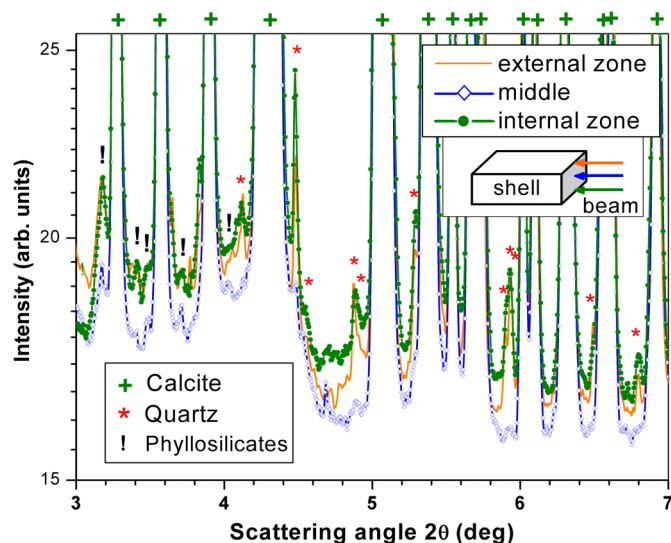

Figure 2 | ML1188 eggshell (a) SEM micrograph of the eggshell radial section (b) optical micrograph eggshell radial section showing acicular crystals and a single layer; (c) SEM micrograph of the external surface of the eggshell, and (d) SEM micrograph of the internal surface of the eggshell.

Figure 3 | SR-μCT image of the eggshell in (a) external, (b) internal and (c) transverse view.

(Fig. 3a). An external zone (Supplementary Note 1) resembling an additional layer may be present in the eggshells. However, the SR-XRD analysis of the external and internal surface zones of the eggshell fragments shows the presence of quartz and phyllosilicates
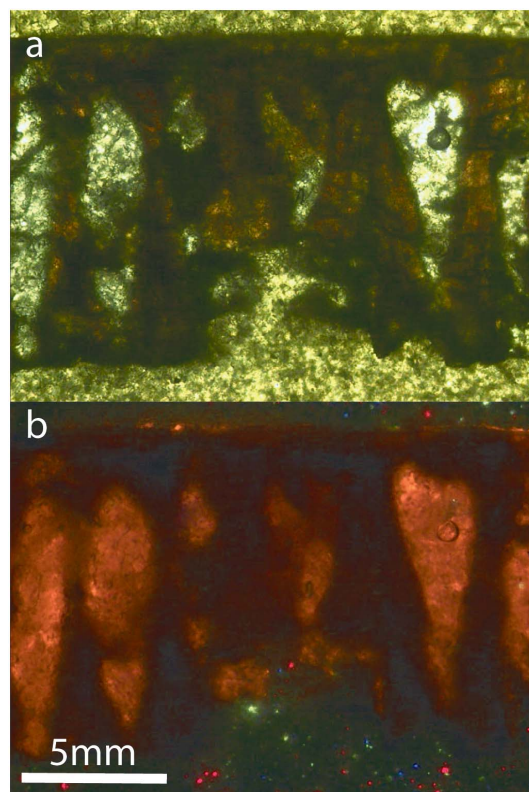

Figure 4 | SR-XRD patterns obtained for an eggshell from ML1188 at the topmost zone (external surface zone), at the middle and at the bottommost zone (internal surface zone) of the eggshell. The data were acquired in transmission mode (beam closely parallel to the outer/inner surfaces of the eggshell). The identification of the compounds present in each zone was performed by comparing the measured SR-XRD patterns with data sets from the PDF-2 database.

(Fig. 4). Furthermore, SR-XRD (Fig. 4) and micro-PIXE (Supplementary Note 8) data indicate that pore-filling sediment is composed mainly of phyllosilicates. SR-XRD shows that the major compound of the eggshell is calcite (Fig. 4). The inner surface shows some degree of flattening, and in some points partial fusion of the mammillae (see upper right corner of Fig. 2d). The eggshells do not luminesce under the impact of accelerated electrons by the CL equipment (Fig. 5). Luminescence is only observed on the pores. The micro-PIXE analysis of the eggshell (excluding pores) revealed the presence of Mg, Fe, Mn, Si (0.33%, 0.27%, 0.18% and 0.10%, respectively) and several trace elements (Na, Al, S, K and Cl), with a corresponding loss of Ca (Table 1, Supplementary Note 8).

Discussion

ML1188 can be assigned to Theropoda due to the presence of strongly elongated, sharply pointed crowns with a distal curvature. Among non-theropod dinosaurs, this condition is only present in the basalmost sauropodomorph *Eoraptor*[20]. Nonetheless, some *Eoraptor* crowns are lanceolate and the maxillary teeth are not so elongated, contrarily to ML1188. Among Theropoda, the antorbital tooth row indicates tetanuran relationships[17] for ML1188. An anteriorly inclined nutrient groove between the medial wall of the maxillary body and the interdental plate, as well as strongly convergent ventral and dorsal margins of the jugal ramus are also two synapomorphies for Megalosauridae (Supplementary Note 3 and 7). We ascribe ML1188 to Megalosaurinae based on the presence of less than ten dentary teeth, from the anteriormost point of the mandibular symphysis to the anteriormost point of the Meckelian fossa, as well as the absence of the internal antorbital fossa on the medial side of the maxilla (Supplementary Note 3, 5 and 7). The maxillary fenestra, promaxillary fenestra and pneumatic recesses appear early in ontogeny and in the maxilla of Tetanurae embryos[9,21]. The maxillary fenestra pierces the maxilla in most tetanurans[22], but corresponds

Figure 5 | Radial section of the eggshell under (a) polarized lens and (b) cathodoluminescence. There is no part of the eggshell that luminesces except on the pores due to the presence of phyllosilicates.

4

Table 1 | Compositional results for the eggshell and pore inclusions as determined by micro-PIXE technique. The remaining percentage includes oxygen and carbon

%w	eggshell	pore inclusions
Na	0.09	0.6
Mg	0.33	1.9
Al	0.09	11.6
Si	0.10	25.2
P	n.d.	0.07
S	0.08	0.09
Cl	0.02	0.08
K	0.03	2.4
Ca	39.4	6.0
Ti	n.d.	0.4
Mn	0.18	0.03
Fe	0.27	3.6

to a small opening located within the internal antorbital fossa in some basal tetanurans[22,23], for example, *Duriavenator* and *Megalosaurus* (Supplementary Note 3). However, as in ML1188, an unfenestrated and unpneumatized maxilla lacking a medial-antorbital fossa is only present in few megalosaurids (e.g., *Torvosaurus*, *Dubreui-llosaurus*, see Supplementary Note 3). The embryonic remains of ML1188 share three synapomorphies with both Megalosaurinae *Megalosaurus* and *Torvosaurus*: a blunt and unexpanded anteroventral margin of the dentary, very elongated maxillary crowns (Crown Height Ratio > 2.5) and tall and unfused anteriormost interdental plates of the dentary (Supplementary Note 3, 5 and 7). This embryo can be referred to the genus *Torvosaurus* due to the lack of pneumaticity posterior to the base of the ascending process, an angle of less than 35° in between the base of the ascending process and the ventral margin of the maxilla, and the tongue-shaped extremity of the jugal ramus of the maxilla. The maxilla of *Megalosaurus* displays two pneumatic excavations on the medial surface of the maxillary body, dorsal to the lingual bar and posterior to the ascending process in medial view[23]. In addition, the angle in between the base of the ascending process and the alveolar margin of the maxilla exceeds 35° and the posterior extremity of the jugal ramus tapers as a very long pointing process. Importantly, *Torvosaurus* has been previously reported from the same Formation in Portugal[24]. Four features differentiate ML1188 from the maxilla of adult *Torvosaurus*: (i) absence of serrations on the mesial and distal carinae, (ii) absence of fusion of the interdental plates in the maxilla, and an (iii) anteroposteriorly short anterior ramus (iv) bearing less than six maxillary teeth. These features are most likely related to morphological variation through ontogeny. The lack of tooth serrations among non-coelurosaur theropods is rare, being only observed in teeth of Spinosaurinae[25]. However, the lack of denticles in portions of the maxillary teeth has been observed in the embryo of the basal avetheropod *Lourinhanosaurus* ML565-122, namely in the mesial and apical portion of the distal carinae. Likewise, the embryonic specimen of *Troodon* also bears unserrated crowns, in contrast to the condition found in adults[9]. ML1188 is the only case of complete absence of serrations known to date in non-coelurosaur theropod embryos. In coelurosaurs, besides *Troodon*, the *Byronosaurus* embryo also lacks serrations as in the adult[9,10]. Separated interdental plates occur in the maxilla in several adult specimens of megalosaurids (e.g., *Megalosaurus*, *Duriavenator*). In the *Torvosaurus* holotype (BYUVP 9122, BYUVP - Brigham Young University Vertebrate Paleontology, Provo, Utah, USA), and a larger maxilla (ML1100) discovered in the Lourinhã Formation, the maxillary interdental plates are completely fused unlike part of the dentary in the holotype of *Torvosaurus* (BYUVP 2003). Unpreserved interdental plates in the hatchling *Allosaurus*[21] may suggest that these elements were unfused

in juveniles, contrary to the condition seen in adult *Allosaurus*. Thus, fusion of interdental plates in the maxilla of basal tetanurans seems to occur after hatchling. Likewise, the proportion of the anterior ramus and the maxillary tooth count have also been previously described as traits that may vary ontogenetically at post-embryonic stages[21]. These four conditions, the absence of denticles, fusion of the maxillary interdental plates, elongation of the anterior ramus and the differences in maxillary tooth counts, are traits that vary trough theropod ontogeny after hatchling.

Preservation of the eggshells ranges from pristine to slightly abraded mammillae, corresponding to Stage 1 of eggshell corrosion[26], and the eggshells show little evidence of bacterial or chemical corrosion[26,27]. The minor flattening of the mammillae can be due to bacterial action, although natural degradation of the eggshell can produce similar results[27]. Furthermore, no corrosion pits or pinholes are present. Other manifestations of very mild diagenesis are the absence of: epitaxial calcite growth blankets, "ghost" crystals, and criss-crossed calcite veins[17,29]. At the micrometer scale, individual calcite grains are distinct and show neither smoothing nor the fibrous texture that has been detected in acidic and/or high temperature conditions in avian eggshells[26]. The external ornamentation of the ML1188 eggshells is distinct from the honeycombed surficial pattern caused by acidic corrosion. The pattern of thin, sharp, straight walls visible in heavily corroded eggshells[26] differs from the broad, meandering and anastomosing external ornamentation of ML1188 eggshells. The putative additional layer detected in some shells (see Results) is due to sediment from the surrounding matrix and does not represent a true secondary layer[15]. In fact, this layer is composed of extrinsic material not pertaining to the eggshell (Fig. 4 and 5, Table 1, Supplementary Note 8 and 9). Thus, from an external morphology perspective there is no evidence of diagenesis. However, diagenesis can affect the eggshell at a chemical level. The non-luminescence of the eggshells (Fig. 5) could imply that there was little to no diagenetic influence on the eggshells. Nevertheless, the quenching effect of Fe^{2+} has to be taken into consideration[29,30] as it may mask the extension of diagenesis. In fact, micro-PIXE revealed trace amounts of Fe as well as other Ca-substituting elements (see Results). Therefore, the minimal presence of these elements and corresponding low loss of Ca in calcite, indicates very mild diagenesis. On the other hand, the luminescence observed on the pores (Fig. 5) is due to the presence of phyllosilicates, which are rich in luminescent elements. The combination of CL and micro-PIXE techniques is thus necessarily complementary. This series of tests indicate that eggshell external morphology has not been altered by diagenetic effects. Diagenesis affected only, very mildly, at a chemical level the eggshell's composition.

The clutch was not significantly taphonomically disturbed (Supplementary Note 1 and 6). There are several facts supporting this statement, namely: (i) the presence of articulated vertebrae, (ii) the concentrated clutch without surrounding dispersed eggshells, (iii) the undisplaced eggshells within the clutch, and (iv) the poorly cemented teeth found *in situ* in the maxilla and dentary, (v) the nest was located in a low energy fluvial overbank setting. However, the preservation of few bone elements seems to be contradictory evidence. This can be explained by the reduced mineralization of embryonic bones, which results in increased degradation and decomposition. This nearly undisturbed taphonomic scenario can be explained by deliberate burial from the progenitor, analogously to the behavior seen in extant seaturtles. Importantly, the eggshells are highly porous. Porous eggshells have high gas and vapor conductance, which allows efficient gaseous exchange between the external and internal media, whereas simple porous systems are indicative of exposed nesting conditions[31]. The eggshells are highly porous and, thus, indicative of eggs buried for incubation within the substrate. ML1188 could have been buried by the progenitor because of the high porosity of the eggshells, undisturbed taphonomic setting, and low-energy geological context.
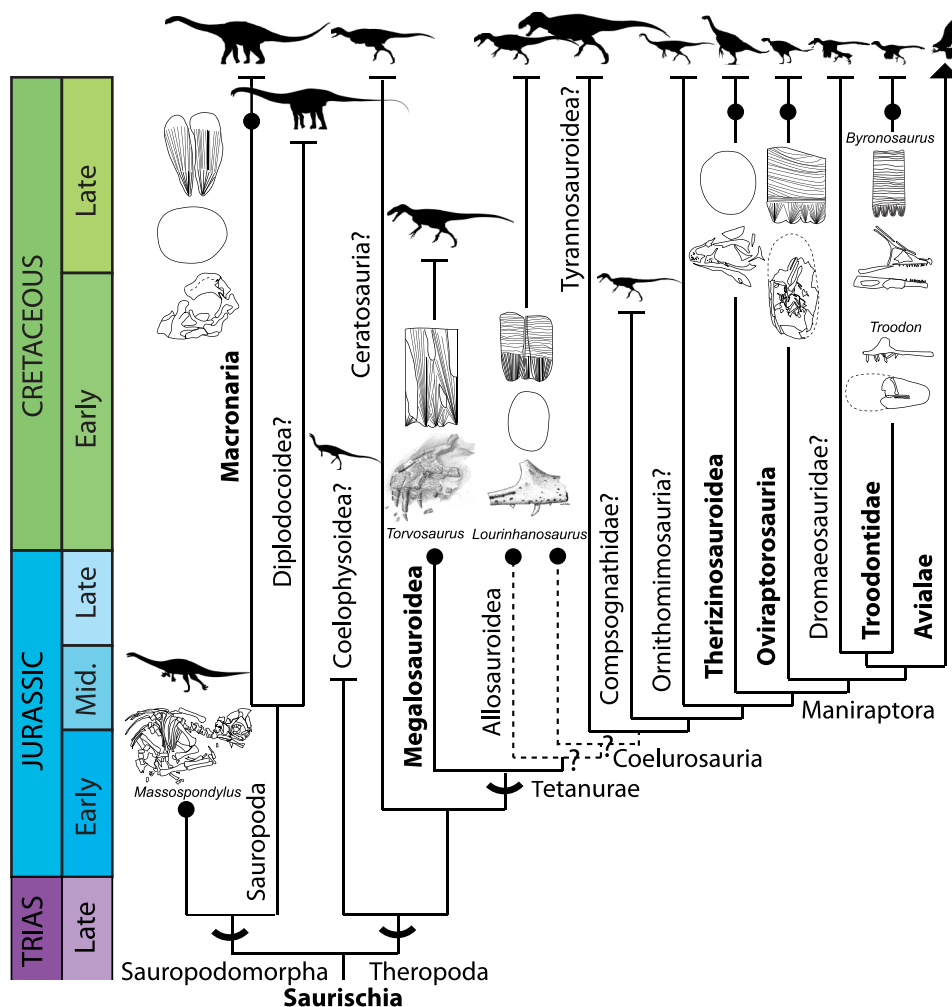
ML1188 eggshells allow ascription to a non-maniraptoran saurischian, based on the derived characters from a previous phylogenetic optimization of egg characters[2]: (i) presence of surficial ornamentation, (ii) acicular crystals as building blocks of the eggshell structure, and (iii) absence of two aprismatic layers. What was previously thought to be a theropod synapomorphy concerning the tubular shape of the pore canals[32], does not hold true considering the prolatocanaliculate-type[1] pores in ML1188. Using parataxonomy, it is difficult to determine whether these eggshells belong to the dinosauroid-spherulitic basic shell type, due to the presence of distinct shell units and boundaries. The ML1188 eggshells are most closely related to the Dendroolithidae oofamily based on the presence of (i) a single eggshell layer, (ii) irregularly shaped shell units, (iii) branching fans, (iv) lack of true mammillae, (v) pore canals forming an intercone space, (vi) prolatocanaliculate type[1,33], and (vii) shell units extending to the surface (prismatic condition). Dendroolithid eggshells have only been reported from the Late Cretaceous of China and Mongolia[33,34], thus, ML1188 represents the first shells of this type known from the Late Jurassic. Dendroolithidae eggshells were thought to be associated with either sauropods or ornithopods[35], but the ML1188 embryos definitively link this type of eggshell to theropods (Fig. 1–3).

Concerning non-theropod taxa, titanosaurid eggshells are composed of one structural layer, whereas. ML1188 eggshells (1.2 mm) are slightly thinner than the 1.8 mm titanosaurid eggshells[37], but the external ornamentation is superficially similar. SEM imaging, optical microscopy and SR-µCT analysis reveals an intricate anastomosing pattern in ML1188 (Fig. 2, 3) that is distinct from the nodular surficial pattern of Titanosauridae eggshells[28]. Furthermore, ultrastructural features reveal a very different pore system and arrangement of shell units. Titanosauridae eggshells have broad open-angled shell units[28], in contrast to ML1188 eggshell units that form a sharp angle where they meet the outer surface, producing its peculiar ornamentation (Supplementary Videos). Also readily excludable are ornithischian eggshells: *Hypacrosaurus sternbergi* eggshells do not have individualized shell units[28], and the neoceratopsid IGM 100/2010 (IGM - Institute of Geology, Ulaan Bataar, Mongolia) possesses several eggshell layers and blade-shaped crystals at the base of the eggshell[13].

Apart from the ML1188 embryos, there are no other reported megalosauroid embryos. This finding not only identifies a unique and previously unknown eggshell morphotype, but more importantly, it bridges a phylogenetic gap at the base of the Theropoda clade (Fig. 6). Nevertheless, it should be noted that the single eggshell layer and acicular morphology are Saurischia synapomorphies[2]. ML1188 eggshells represent the first report of theropod eggs with a single structural layer, the plesiomorphic condition for Theropoda. The two non-coelurosaurian tetanuran taxa, *Lourinhanosaurus*

Figure 6 | The known record of embryos and associated eggshell structure explicits the phylogenetic position of the *Torvosaurus* embryos (ML1188), which occupies a gap at the base of the Theropoda cladogram. Dashed lines indicate the dubious position of *Lourinhanosaurus* as an Allosauroidea or as a basal Coelurosauria in the light of the most recent analysis[17]. Major clades in bold indicate the presence of associated embryo-eggshell fossils. For attribution information on the individual elements of this figure please see the Supplementary Information.

antunesi ML565 and *Torvosaurus* ML1188, have clearly distinct eggshell morphotypes. ML1188 eggshells differ from those tentatively ascribed to *Lourinhanosaurus antunesi* because the later (i) lack ornamentation, (ii) exhibit a tubular and oblique pore system, (iii) are thinner (average = 0.92 mm)[36]. Moreover, eggshells assigned to *Lourinhanosaurus antunesi* bear two distinct layers, and the basal layer displays large nucleation centers[18]. Although the ML1188 embryos and those assigned to *Lourinhanosaurus antunesi* are morphologically similar and closely related phylogenetically, they have strikingly different eggshell morphologies. The marked difference in the eggshells of these two taxa implies that the taxonomic assignment of ML565 to *Lourinhanosaurus antunesi* can be either incorrect, or eggshell characters are highly homoplastic in basal theropods, or the phylogenetic position of *Lourinhanosaurus antunesi* is uncertain, probably being an Allosauroidea or basal Coelurosauria[17]. Ongoing research on the ML565 embryos is attempting to resolve this issue. ML1188 eggshells are different from those of the coelurosaur *Troodon formosus*. The later, with an average thickness of 1.02 mm, exhibit (i) two structural layers, (ii) pores with a constant diameter, and (iii) spherulites composed of blade-like calcite crystals. The other coelurosaur theropods can be readily excluded because oviraptosaurids and ML565 are composed of two structural layers, and Avialae eggshells have three layers[2].

Methods

Geology. The Lourinhã Formation is located on the west coast of Portugal in the Lusitanian Basin, a rift structure that formed during the opening of the proto-North Atlantic in the Jurassic[38]. The Upper Jurassic Lourinhã Formation was deposited during a period of global sea level rise and concomitant local subsidence[39]. The resultant increase in accommodation space facilitated development of coastal meandering fluvial and delta fan environments punctuated by brief marine incursions[40]. Abundant dinosaur bones and tracks, as well as fossil remains of other continental vertebrates, are an important component of the fauna in this formation[40]. The Sobral Member of the Lourinhã Formation is composed of deltaic sandstones and mudstones[41] (Supplementary Note 10). The Sobral Member is early Tithonian in age, based on stratigraphic correlation, vertebrate and invertebrate (chiefly bivalves and gastropods) biostratigraphy, and Sr-isotope chemostratigraphy using oyster shells[41,42]. The layer from which the clutch was collected is approximately 35 m above the Kimmeridgian-Tithonian boundary[41] (152.1 ± 0.9 Ma[43]) (Supplementary Note 10).

Eggshell characterization. An analysis of the general morphology, microstructure, and elemental composition of fossil eggshell as well as the identification of the compounds present is necessary to provide pertinent information about the extent of diagenesis affecting external morphology and the nest environment in which eggshells are preserved. Optical microscopy was employed to study thin-sections sliced radially and transversely from several eggshell fragments. The observations were performed using a Zeiss Axioplan 2 polarized light microscope and a coupled Nikon DXM200F digital camera. For the preparation of the samples, eggshell fragments were placed on a silicone or clay mould that was subsequently filled with epoxy glue. The hardened block was then glued with epoxy to a microscope slide, sectioned using a diamond disk Struers Discoplan-TS, and subsequently abraded with fine sandpaper until the thickness allowed light to be transmitted. Finally, the sample was polished with a Buehler PETROPOL until thin-sections reached an optimized thickness for analysis on the polarized lens microscope. Furthermore, a lumic HC3-LM cathodoluminescence microscope was used to study the luminescence of the polished thin section surfaces irradiated by an electron beam (the microscope is equipped with a tungsten filament). SEM was also used to characterize the eggshell fragments. Observations were carried out on a JEOL JSM-T330A microscope using an accelerating voltage of 20 kV. For this purpose, the samples were cleaned in an ultrasonic bath for 5 min and subsequently coated with gold. Cross-sectional SEM micrographs and micrographs of the outer and inner surfaces of the eggshell were collected. SR-μCT studies were performed at the beamline HARWI II operated by the Helmholtz-Zentrum Geesthacht (HZG) at the storage ring DORIS III at the Deutsches Elektronen-Synchrotron (DESY) in Hamburg, Germany. The samples were imaged in absorption mode with photon energy of 37 keV. For acquiring the X-ray attenuation projections, the sample was rotated between -180° and 180° in equidistant steps of 0.2°. Technical details of the beamline are described elsewhere[44]. For the evaluation of the SR-μCT data, slices perpendicular to the rotation axis were reconstructed from the single projections by a tomographic reconstruction algorithm using "filtered backprojection". The slices were then collected in an image stack that can be visualized, edited and exported into different file formats using a three-dimensional rendering software. Visualization of the morphology of the samples was conducted using VGStudio Max 1.2.1 (Volume Graphics, Heidelberg, Germany) and TOMO-GPU (Project PTDC/EIA-EIA/102579/2008). The effective pixel size corresponds to 6.4 μm. The

High Energy Materials Science beamline (HEMS)[45] at the storage ring PETRA III at DESY offers the opportunity to investigate fine structural details (high flux in parallel beam to increase resolution and enough signal in the small gauge volumes). Eggshell fragments were broken into pieces of approximately 5 × 5 mm in order to obtain samples exhibiting "fresh" cross-sections. SR-XRD data were acquired at HEMS in transmission mode (with an image plate MAR345) using a beam spot of 100 μm in vertical and 300 μm in horizontal with 87 keV energy (the eggshell fragments were mounted on the sample holder with the outer and inner shell surfaces nearly parallel to beam). The samples were measured starting from the outer surface to the inner surface of the shell, along a "line" (width = 300 μm) perpendicular to these surfaces, every 100 μm with an acquisition time of 1 s. The compounds present in each zone were identified by comparing the experimental data with data sets from a Powder Diffraction File database (PDF-2) maintained by the International Center for Diffraction Data (ICDD). Micro-PIXE analysis was used to identify and map the elemental composition of eggshell samples within micron-scale regions. The experiments were performed at IST/CTN – Campus Tecnológico e Nuclear, Portugal. The Ion Beam Laboratory is equipped with a 2.5 MV Van de Graaff accelerator and an ion microprobe (Oxford Microbeams) with focused beam providing approximately 3 μm spatial resolution. The scanning nuclear microprobe was used to obtain two-dimensional X-ray elemental distribution maps in cross-section analysis of eggshell fragments. During the experiments the sample was exposed to a proton beam (an area of 1860 × 1860 μm) with an energy of 1 MeV, which provided information about the shell and pores composition.

1. Carpenter, K. *Eggs, nests and baby dinosaurs: A look at dinosaur reproduction.* (Indiana Press, 1999).
2. Grellet-Tinner, G., Chiappe, L. M., Norell, M. & Bottjer, D. Dinosaur eggs and nesting behaviors: a paleobiological investigation. *Palaeogeogr. Palaeoclimatol. Palaeoecol.* **232**, 294–321 (2006).
3. Grellet-Tinner, G. *et al.* Description of the first lithostrotian titanosaur embryo in ovo with Neutron characterization and implications for lithostrotian Aptian migration and dispersion. *Gondwana Res.* **20**, 621–629 (2011).
4. Reisz, R. R., Evans, D. C., Sues, H.-D. & Scott, D. Embryonic skeletal anatomy of the sauropodomorph dinosaur *Massospondylus* from the Lower Jurassic of South Africa. *J. Vertebr. Paleontol* **30**, 1653–1665 (2010).
5. Mateus, I. *et al.* Upper Jurassic Theropod Dinosaur embryos from Lourinhã (Portugal) Upper Jurassic paleoenvironments in Portugal. *Mem. Acad. Ciênc. Lisb.* **37**, 101–109 (1998).
6. de Ricqlès, A., Mateus, O., Antunes, M. T. & Taquet, P. Histomorphogenesis of embryos of Upper Jurassic theropods from Lourinhã (Portugal). *C. R. Acad. Sci., Series IIA-Earth Planet. Sci.* **332**, 647–656 (2001).
7. Kundrát, M., Cruickshank, A. R. I., Manning, T. W. & Nudds, J. Embryos of therizinosauroid theropods from the Upper Cretaceous of China: diagnosis and analysis of ossification patterns. *Acta Zool. (Stockh.)* **89**, 231–251 (2008).
8. Salgado, L., Coria, R. A. & Chiappe, L. M. Osteology of the sauropod embryos from the Upper Cretaceous of Patagonia. *Acta Palaeontol. Polonica* **50**, 79–92 (2005).
9. Varricchio, D. J., Horner, J. R. & Jackson, F. D. Embryos and eggs for the cretaceous theropod dinosaur *Troodon formosus*. *J. Vertebr. Paleontol* **22**, 564–576 (2002).
10. Beaver, G. B. & Norell, M. A. The perinate skull of *Byronosaurus* (Troodontidae) with observations on the cranial ontogeny of paravian theropods. *Am. Mus. Nov.* **3657**, 1–51 (2009).
11. Norell, M. A., Clark, J. M. & Chiappe, L. M. An embryonic oviraptorid (Dinosauria: Theropoda) from the Upper Cretaceous of Mongolia. *Am. Mus. Novit.* **3315**, 1–17 (2001).
12. Long, J. A. & McNamara, K. J. Heterochrony: The key to dinosaur evolution. in The Dinofest International (Wolberg, D.L., Stump, E. & Rosenberg, G. D., eds.) 113–123 (*Acad. Nat. Sci. Phil.*, 1997).
13. Balanoff, A. M., Norell, M. A., Grellet-Tinner, G. & Lewin, M. R. Digital preparation of a probable neoceratopsian preserved within an egg, with comments on microstructural anatomy of ornithischian eggshells. *Naturwissenschaften* **95**, 493–500 (2008).
14. Varricchio, D. J. *et al.* Avian paternal care had dinosaur origin. *Science* **322**, 1826–1828 (2008).
15. Grellet-Tinner, G. Phylogenetic interpretation of eggs and eggshells: implications for phylogeny of Palaeognathae. *Alcheringa* **30**, 141–182 (2006).
16. Araújo, R., Mateus, O., Walen, A. & Christiansen, N. Preparation techniques applied to a stegosaurian dinosaur from Portugal. *J. Paleontol. Tech.* **5**, 1–23 (2009).
17. Carrano, M. T., Benson, R. B. J. & Sampson, S. D. The phylogeny of Tetanurae (Dinosauria: Theropoda). *J. Syst. Palaeont* **10**, 211–300 (2012).
18. Grellet-Tinner, G. & Makovicky, P. A possible egg of the dromaeosaur *Deinonychus antirrhopus*: phylogenetic and biological implications. *Can. J. Earth Sci.* **43**, 705–719 (2006).
19. Jackson, F. D., Horner, J. R. & Varricchio, D. J. A study of a *Troodon* egg containing embryonic remains using epifluorescence microscopy and other techniques. *Cretac. Res.* **31**, 255–262 (2010).

20. Sereno, P. C., Forster, C. A., Rogers, R. R. & Monetta, A. M. Primitive dinosaur skeleton from Argentina and the early evolution of Dinosauria. *Nature* **361**, 64–66 (1993).

21. Rauhut, O. W. M. & Fechner, R. Early development of the facial region in a non-avian theropod dinosaur. *Proc. R. Soc. B* **272**, 1179–1183 (2005).

22. Witmer, L. M. The evolution of the antorbital cavity of archosaurs: A study in soft-tissue reconstruction in the fossil record with an analysis of the function of pneumaticity. *J.Vertebr. Paleontol* **17**, 1–76 (1997).

23. Benson, R. B. J. A description of *Megalosaurus bucklandii* (Dinosauria: Theropoda) from the Bathonian of the UK and the relationships of Middle Jurassic theropods. *Zool. J. Linn. Soc.* **158**, 882–935 (2009).

24. Mateus, O., Walen, A. & Antunes, M. T. The large theropod fauna of the Lourinhã Formation (Portugal) and its similarity to the Morrison Formation, with a description of a new species of *Allosaurus. N. Mex. Mus. Nat. Hist. Sci. Bull.* **36**, 123–129 (2006).

25. Sues, H.-D., Frey, E., Martill, D. M., Scott, D. M. *Irritator challengeri*, a spinosaurid (Dinosauria: Theropoda) from the Lower Cretaceous of Brazil. *J. Vertebr. Paleontol* **22**, 535–547 (2002).

26. Clayburn, J. K., Smith, D. L. & Hayward, J. L. Taphonomic effects of pH and temperature on extant avian dinosaur eggshell. *PALAIOS* **19**, 170–177 (2004).

27. Smith, D. L. & Hayward, J. L. Bacterial decomposition of avian eggshell: a taphonomic experiment. *PALAIOS* **25**, 318–326 (2010).

28. Grellet-Tinner, G. & Chiappe, L. M. Dinosaur eggs and nestings: implications for understanding the origin of birds. In Feathered Dragons: Studies on the Transition from Dinosaurs to Birds (Currie, P.J., Koppelhus, E.B., Shugar M.A., Wright, J.L., eds.) 185–214 (Indiana Univ. Press, 2004).

29. Budd, D. A., Hammes, U. & Ward, W. B. Cathodoluminescence in calcite cements: new insights on Pb and Zn sensitizing, Mn activation, and Fe quenching at low trace-element concentrations. *J. Sed. Res.* **70**, 217–226 (2000).

30. Savard, M. M., Veizer, J. & Hinton, R. Cathodoluminescence at low Fe and Mn concentrations: a SIMS study of zones in natural calcites. *J. Sed. Res.* **A65**, 208–213 (1995).

31. Seymour, R. S. Dinosaur Eggs: Gas conductance through the shell, water loss during incubation and clutch size. *Paleobiol* **5**, 1–11 (1979).

32. Zelenitzky, D. K. & Therrien, F. Phylogenetic analysis of reproductive traits of maniraptoran theropods and its implications for egg parataxonomy. *Paleontol* **51**, 807–816 (2008).

33. Zhao, Z. & Li, Z. A new structural type of the dinosaur eggs from Anlu County, Hubei Province. *Vert. PalAsiat* **26**, 107–115 (1988).

34. Mikhailov, K. E. Classification of fossil eggshells of amniotic vertebrates. *Acta Palaeontol. Polonica* **36**, 193–238 (1991).

35. Hirsch, K. F. Upper Jurassic eggshells from the Western Interior of North America. In *Dinosaur Eggs and Babies* (Carpenter, K., Hirsch, K.F., Horner, J.R., eds) 137–150 (Cambridge Univ. Press, 1994).

36. Antunes, M. T., Taquet, P. & Ribeiro, V. Upper Jurassic dinosaur and crocodile eggs from Paimogo nesting site (Lourinhã- Portugal). *Mem. Acad. Ciênc. Lisb.* **37**, 83–100 (1998).

37. Grellet-Tinner, G., Chiappe, L. M. & Coria, R. Eggs of titanosaurid sauropods from the Upper Cretaceous of Auca Mahuevo (Argentina). *Can. J. Earth Sci.* **41**, 949–960 (2004).

38. Carvalho, J. *et al.* The structural and sedimentary evolution of the Arruda and Lower Tagus sub-basins, Portugal. *Mar. Petroleum Geol.* **22**, 427–453 (2005).

39. Leinfelder, R. R. Facies, stratigraphy and paleogeographic analysis of Upper? Kimmeridgian to Upper Portlandian sediments in the environs of Arruda dos Vinhos, Estremadura, Portugal. *Münchner Geowiss. Abh. A* **7,** 1–216 (1986).

40. Hill, G. Distal alluvial fan sediments from the Upper Jurassic of Portugal: controls on their cyclicity and channel formation. *J. Geol. Soc., London* **146**, 539–555 (1989).

41. Schneider, S., Fürsich, F. T. & Werner W. Sr-isotope stratigraphy of the Upper Jurassic of central Portugal (Lusitanian Basin) based on oyster shells. *Int. J. Earth Sci.* **98**, 1949–1970 (2008).

42. Mateus, O. Late Jurassic dinosaurs from the Morrison Formation, the Lourinhã and Alcobaça Formations (Portugal), and the Tendaguru Beds (Tanzania): a comparison. *N. Mex. Mus. Nat. Hist. Sci. Bull* **36**, 223–231 (2006).

43. Gradstein, F. M., Ogg, J. G., Schmitz, M. D. & Ogg, G. M. The Geologic Time Scale 2012 Vol. 1, 1–1144 (Elsevier, 2012).

44. Reimers, W., Pyzalla, A. R., Schreyer, A. & Clemens, H. Neutrons and synchrotron radiation in engineering materials science: from fundamentals to material and component characterization. *Wiley-VCH Verlag, Weinheim* (2008).

45. Schell, N. *et al.* The high energy materials science beamline (HEMS) at PETRA III. *AIP Conf. Proc.* **1234**, 391–394 (2010).

Acknowledgements

Author contributions

R.A., R.C., R.M., C.H., manuscript writing and figure preparation; R.A., R.C., thin-sections and S.E.M.; R.M., R.C., F.B., synchrotron data acquisition and imaging; R.M., L.A., micro-PIXE analysis; R.M. and N.S., synchrotron radiation-based x-ray diffraction; C.H., R.A., anatomical description and phylogenetic analysis; R.C., cathodoluminescence; R.A., O.M., geology; R.A., R.C. and O.M., fossil preparation and excavation.

Additional information

Supplementary information accompanies this paper at http://www.nature.com/scientificreports

How to cite this article: Araújo, R. *et al.* Filling the gaps of dinosaur eggshell phylogeny: Late Jurassic Theropod clutch with embryos from Portugal. *Sci. Rep.* **3**, 1924; DOI:10.1038/srep01924 (2013).